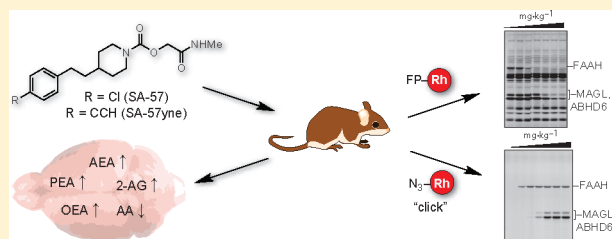


# O-Hydroxyacetamide Carbamates as a Highly Potent and Selective Class of Endocannabinoid Hydrolase Inhibitors

Micah J. Niphakis,<sup>†</sup> Douglas S. Johnson,<sup>‡</sup> T. Eric Ballard,<sup>‡</sup> Cory Stiff,<sup>‡</sup> and Benjamin F. Cravatt<sup>\*,†</sup><sup>†</sup>The Skaggs Institute for Chemical Biology and Department of Chemical Physiology, The Scripps Research Institute, 10550 North Torrey Pines Road, La Jolla, California 92037, United States<sup>‡</sup>Pfizer Worldwide Research and Development, Groton, Connecticut 06340, United States

**ABSTRACT:** The two major endocannabinoid transmitters, anandamide (AEA) and 2-arachidonoylglycerol (2-AG), are degraded by distinct enzymes in the nervous system, fatty acid amide hydrolase (FAAH) and monoacylglycerol lipase (MAGL), respectively. FAAH and MAGL inhibitors cause elevations in brain AEA and 2-AG levels, respectively, and reduce pain, anxiety, and depression in rodents without causing the full spectrum of psychotropic behavioral effects observed with direct cannabinoid receptor-1 (CB1) agonists. These findings have inspired the development of several classes of endocannabinoid hydrolase inhibitors, most of which have been optimized to show specificity for either FAAH or MAGL or, in certain cases, equipotent activity for both enzymes. Here, we investigate an unusual class of *O*-hydroxyacetamide carbamate inhibitors and find that individual compounds from this class can serve as selective FAAH or dual FAAH/MAGL inhibitors *in vivo* across a dose range (0.125–12.5 mg kg<sup>-1</sup>) suitable for behavioral studies. Competitive and click chemistry activity-based protein profiling confirmed that the *O*-hydroxyacetamide carbamate SA-57 is remarkably selective for FAAH and MAGL *in vivo*, targeting only one other enzyme in brain, the additional 2-AG hydrolase ABHD6. These data designate *O*-hydroxyacetamide carbamates as a versatile chemotype for creating endocannabinoid hydrolase inhibitors that display excellent *in vivo* activity and tunable selectivity for FAAH-anandamide versus MAGL (and ABHD6)-2-AG pathways.

**KEYWORDS:** Activity-based protein profiling, anandamide, 2-arachidonoylglycerol, carbamate, endocannabinoid, hydrolase



The endocannabinoid (EC) signaling system regulates a wide range of physiological functions, including mood, appetite, pain sensation, inflammation, locomotion, and memory.<sup>1–5</sup> The EC system consists of two endogenous lipid transmitters, *N*-arachidonoyl ethanolamine or anandamide (AEA) and 2-arachidonoylglycerol (2-AG), their cognate G-protein coupled receptors, CB1 and CB2, and the enzymes responsible for AEA and 2-AG biosynthesis and degradation. The CB1 and CB2 receptors are also the sites of action for  $\Delta^9$ -tetrahydrocannabinol (THC), the principal psychoactive component of marijuana.<sup>5</sup> THC and other direct CB agonists have demonstrated clinical utility for the treatment of pain, sleep, and other nervous system disorders, but also produce undesirable neurological side effects that include weight gain, disruptions in motor control, and cognitive impairment. The pleiotropic nature of the EC system suggests that such side effects may be an inherent liability of direct agonists that globally activate CB1 receptors throughout the organism.

An alternative and potentially more selective strategy to harness the clinical potential of the EC system would be to block the enzymes that terminate AEA and 2-AG signaling *in vivo*.<sup>6,7</sup> Such EC degradation inhibitors might potentiate EC signaling in specific neural circuits to produce a therapeutically useful subset of the behavioral effects caused by direct CB1 agonists. Preclinical studies with selective FAAH inhibitors have provided support for this model, as these agents produce

analgesic,<sup>8–14</sup> anti-inflammatory,<sup>15–17</sup> anxiolytic,<sup>12,18,19</sup> and antidepressant<sup>18,20</sup> effects in the absence of motor or cognitive impairment. A similar pattern of phenotypes is observed in FAAH<sup>-/-</sup> mice.<sup>8,11</sup> Selective MAGL inhibitors, such as the carbamate JZL184, have only recently been developed<sup>21,22</sup> and are therefore less well-studied, but appear to produce a broader array of cannabinoid effects in rodents that nonetheless still avoid the psychotropic activity of direct CB1 agonists.<sup>23</sup> Complete pharmacologic or genetic blockade of MAGL for extended periods of time also leads to behavioral tolerance and desensitization of brain CB1 receptors,<sup>24</sup> but these adaptations can be avoided with lower doses of JZL184 that produce chronic, partial inhibition of MAGL.<sup>25,26</sup> Collectively, these studies suggest that selective FAAH or MAGL inhibitors have the potential to produce the desired analgesic and anxiolytic/antidepressant effects of direct CB1 agonists while avoiding their major psychotropic side effects.

FAAH inhibitors fall into two major classes: reversible and irreversible (Figure 1).<sup>2,27–29</sup> Although several highly potent

**Special Issue:** Therapeutic Potential of Endocannabinoid Metabolic Enzymes

**Received:** September 22, 2011

**Accepted:** October 10, 2011

**Published:** October 10, 2011

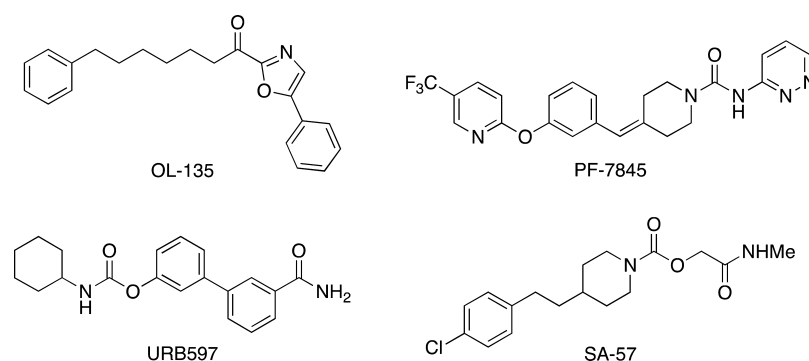
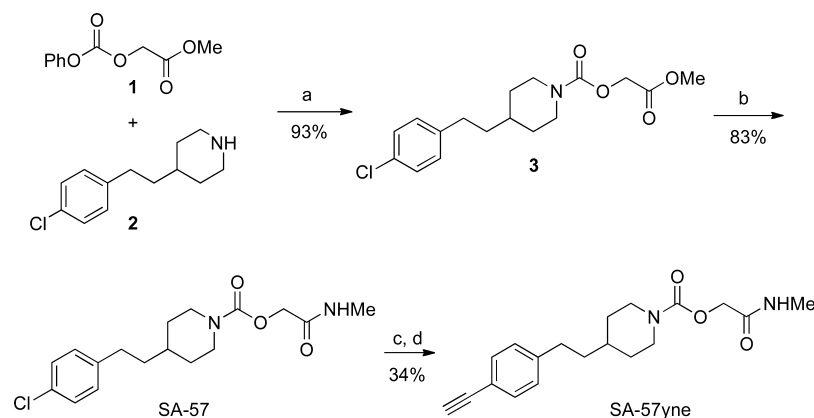


**Figure 1.** Representative structures of reversible and irreversible FAAH inhibitors.

### Scheme 1. Synthesis of SA-57 and SA-57yne<sup>a</sup>



<sup>a</sup>(a) DIEA, DMSO, 60 °C; (b) 2 M MeNH<sub>2</sub> in THF, DMSO; (c) triethylsilylacetylene, PdCl<sub>2</sub>(CH<sub>3</sub>CN)<sub>2</sub>, X-Phos, CH<sub>3</sub>CN, 85 °C; (d) TBAF, THF, 0 °C.

and selective reversible FAAH inhibitors have been developed (e.g., OL-135<sup>9</sup>), sustained elevation of AEA *in vivo* has only been achieved with a handful of these agents. Many additional classes of irreversible FAAH inhibitors have been described; however, honing the selectivity of irreversible inhibitors toward FAAH and away from over 200 human serine hydrolase off-targets presents a formidable challenge. Despite this obstacle, potent and selective irreversible FAAH inhibitors have been developed and are currently under clinical investigation (e.g., PF-04457845, or PF-7845, Pfizer; Figure 1).<sup>30,31</sup> These agents are carbamates and ureas, which inactivate FAAH through carbamylation of catalytic Ser241.<sup>32–36</sup> Although the essential feature of these inhibitors is an electrophilic carbonyl group, potency and selectivity is also dependent on the initial noncovalent binding event.<sup>37</sup>

A broad survey of the most potent and selective carbamate and urea FAAH inhibitors reveals that they almost exclusively contain *O*-aryl or *N*-aryl leaving groups,<sup>27,28</sup> which might, by itself, suggest a minimal requirement for reactivity. One notable exception is a class of *O*-hydroxyacetamide carbamates originally disclosed in patents filed by Sanofi-Aventis.<sup>28,38</sup> Beyond their structural novelty, the absence of published pharmacological data on these compounds motivated us to investigate the *O*-hydroxyacetamide carbamate chemotype. In doing so, we have found that one of these agents, SA-57 (Figure 1), is a remarkably potent FAAH inhibitor with *in vivo* efficacy at doses as low as 0.05 mg kg<sup>-1</sup>. We further determined by competitive activity-based protein profiling (ABPP)<sup>39</sup> that SA-57 also inhibits the 2-AG hydrolases MAGL and ABHD6,

but not other brain serine hydrolases, at doses within 25-fold of that required for FAAH inhibition. These findings thus designate the *O*-hydroxyacetamide carbamate as a privileged chemotype for designing inhibitors that show excellent *in vivo* activity and tunable selectivity for endocannabinoid hydrolases.

## RESULTS AND DISCUSSION

**Synthesis of SA-57 and SA-57yne.** SA-57 was prepared according to Scheme 1. Commercially available 4-(4-chlorophenethyl)piperidine (**2**) was acylated with methyl 2-((phenoxy)oxy)acetate (**1**) to give carbamate **3**, which was treated with methylamine to provide SA-57. We also prepared a clickable analogue of SA-57, SA-57yne, in order to facilitate *in vivo* analyses of selectivity (see below). SA-57yne was accessible in two steps from SA-57 using Sonogashira cross-coupling conditions<sup>40</sup> with triethylsilylacetylene and subsequent removal of the triethylsilyl group with TBAF.

**In Vitro Characterization of SA-57 as an Endocannabinoid Hydrolase Inhibitor.** We first evaluated SA-57 for its activity against serine hydrolases in the mouse brain membrane proteome by competitive-ABPP.<sup>39</sup> In this method, proteomes are first treated with an inhibitor and then the general serine hydrolase activity-based probe fluorophosphonate-rhodamine (FP-Rh).<sup>41,42</sup> Reductions in FP-Rh labeling identify serine hydrolases that are sensitive to the test inhibitor. Competitive ABPP revealed that SA-57 is a highly potent inhibitor of FAAH with an IC<sub>50</sub> < 10 nM (Figure 2). At higher concentrations (10 μM), SA-57 also inhibited two additional brain serine hydrolases, the 2-AG-metabolizing enzymes MAGL and

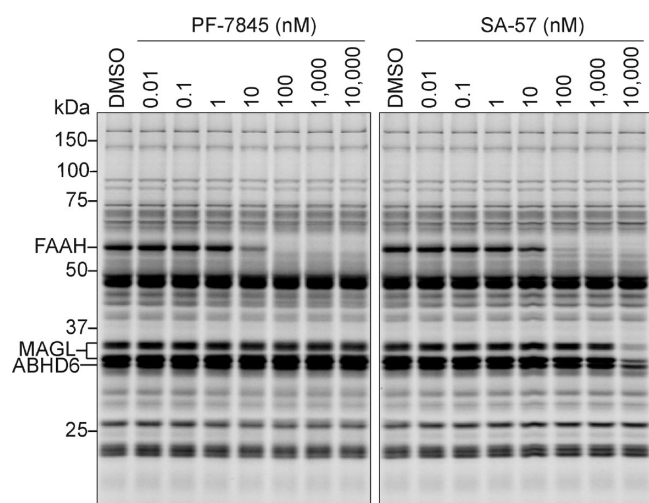


**Figure 2.** Concentration dependent, in vitro competitive ABPP analysis of PF-7845 and SA-57 in the mouse brain membrane proteome using the serine hydrolase-directed probe FP-Rh. PF-7845 selectively blocks FP-Rh labeling of FAAH across the full inhibitor concentration range tested, whereas SA-57 selectively blocks labeling of FAAH at lower concentrations (10 nM to 1  $\mu$ M), but also inhibits MAGL and ABHD6 at higher concentrations (10  $\mu$ M).

ABHD6.<sup>43,44</sup> For comparison, we also evaluated the urea PF-7845, which, consistent with previous reports,<sup>30,31</sup> potently ( $IC_{50} < 10$  nM) and selectively inactivated FAAH.

We next confirmed the activity of SA-57 toward human and mouse FAAH, MAGL, and ABHD6 orthologues assayed as recombinantly expressed proteins in transfected HEK293 cell proteomes by competitive ABPP (Figure 3). Both human and mouse FAAH enzymes were equipotently inhibited by SA-57 with  $IC_{50}$  values of 1–3 nM. Similar  $IC_{50}$  values were obtained

for PF-7845. We should note that these  $IC_{50}$  values may approach the concentration of FAAH enzymes in the assayed proteomes and therefore represent lower limits of potency for SA-57 and PF-7845. At higher concentrations, SA-57, but not PF-7845, also inhibited mouse ( $IC_{50} = 410$  nM) and human ( $IC_{50} = 1.4$   $\mu$ M) MAGL. Human and mouse ABHD6 share >90% sequence identity, and therefore, we only evaluated the mouse orthologue of this enzyme, which was inhibited by SA-57 ( $IC_{50} = 850$  nM) but not by PF-7845 (Figure 3c).

O-Aryl carbamate and N-aryl urea inhibitors have been shown to irreversibly inhibit FAAH by carbamylation of the enzyme's serine nucleophile.<sup>32–36</sup> A feature of such irreversible inhibitors is the time-dependent inactivation of FAAH.<sup>45</sup> To test whether SA-57 also acted through an irreversible mechanism, we determined the extent of endocannabinoid hydrolase inhibition at 10 min intervals over a 40 min reaction period by competitive ABPP. SA-57, like the characterized irreversible inhibitors PF-7845 and JZL184, exhibited clear time-dependent inhibition of FAAH and MAGL (Figure 4), suggesting a covalent mechanism of inactivation, presumably through carbamylation of the active site serine nucleophiles of these enzymes.

**In Vivo Characterization of SA-57 as an Endocannabinoid Hydrolase Inhibitor.** We next determined whether SA-57 could inhibit endocannabinoid hydrolases in vivo. C57Bl/6 mice were treated with a dose range (0.01–12.5 mg  $kg^{-1}$ , i.p.) of SA-57 or PF-7845 for 2 h and then sacrificed, and their brain proteomes analyzed by competitive ABPP in comparison to brain proteomes from vehicle-treated control mice (Figure 5). PF-7845 and SA-57 showed overlapping, but distinct dose-responsive activity against brain serine hydrolases. Consistent with previous studies,<sup>30,31</sup> PF-7845 completely inhibited brain FAAH at doses as low as 0.05 mg  $kg^{-1}$ . SA-57 also partially inhibited FAAH at this dose, but required higher

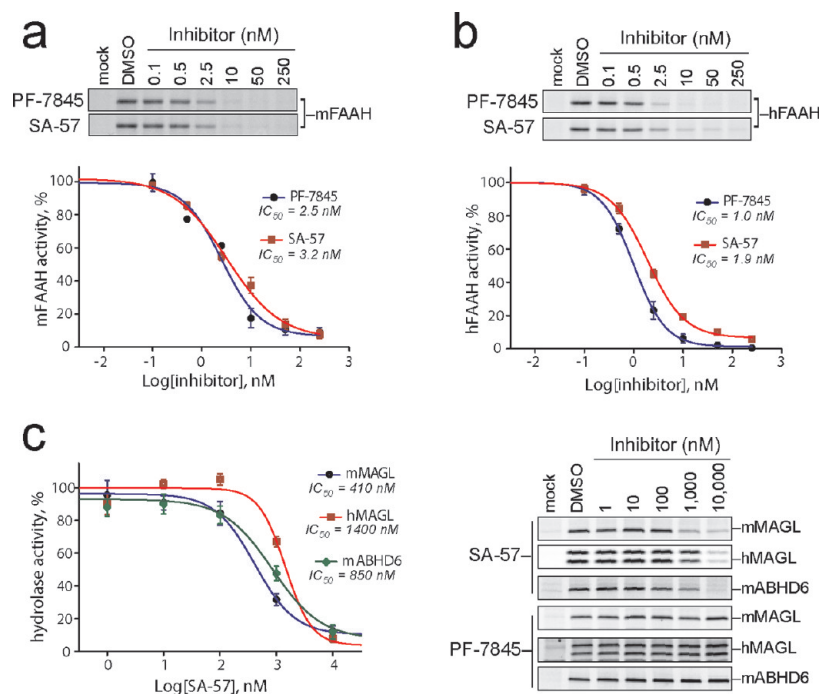


**Figure 3.** Concentration dependent, in vitro competitive ABPP analysis of PF-7845 and SA-57 against recombinant human and mouse FAAH, MAGL, and ABHD6 enzymes expressed by transient transfection in HEK293 cells. Inhibitory activity against (a) mFAAH, (b) hFAAH, and (c) mMAGL, hMAGL, and mABHD6.



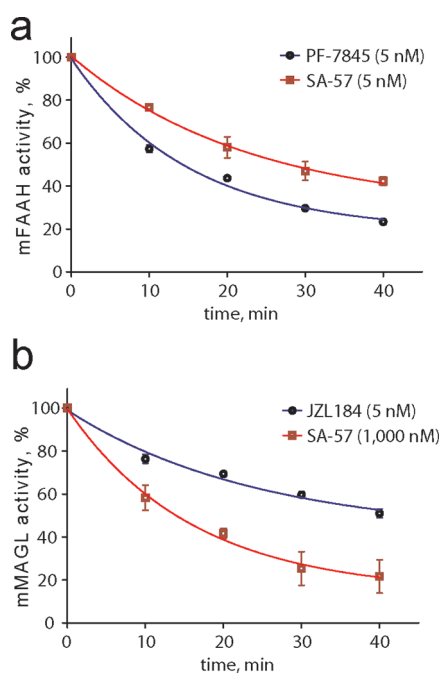


**Figure 4.** Time-dependent inhibition of mouse FAAH (a) and MAGL (b) enzymes by PF-7845, SA-57, and JZL184 as determined by competitive ABPP.

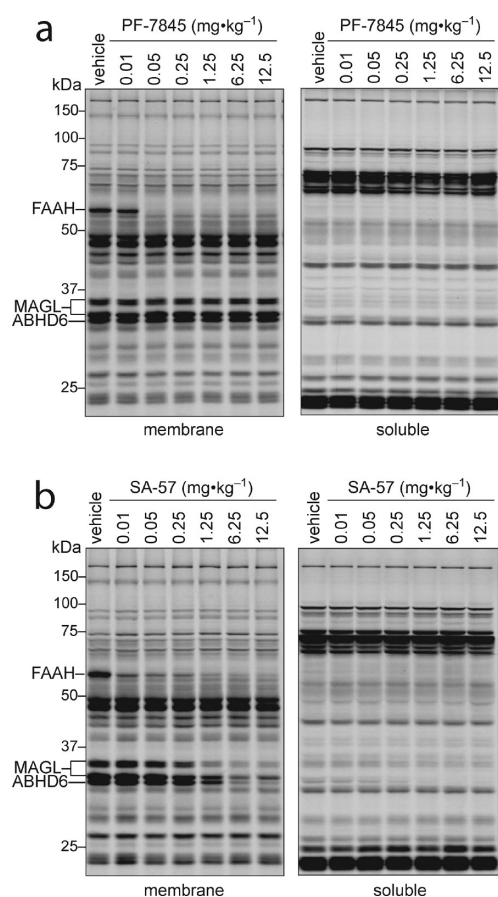


**Figure 5.** Competitive ABPP of brain serine hydrolase activities from mice treated with PF-7845 (a) and SA-57 (b) at the indicated doses (0.01–12.5 mg kg<sup>-1</sup>, i.p.) for 2 h.

doses ( $\geq 1.25$  mg kg<sup>-1</sup>) to inactivate >95% of FAAH activity. As predicted from our in vitro competitive ABPP studies, SA-57, but not PF-7845, also inhibited MAGL and ABHD6 in vivo, with  $\sim 50\%$  reductions in these enzyme activities being observed at the 1.25 mg kg<sup>-1</sup> dose of SA-57 and near complete blockade at a dose of 12.5 mg kg<sup>-1</sup>. Other brain serine hydrolases were not affected by SA-57, indicating that it is a selective inhibitor of the endocannabinoid hydrolases FAAH, MAGL, and ABHD6.

**A Clickable Probe to Directly Evaluate SA-57-Modified Proteins in Vivo.** While our competitive ABPP studies suggested that SA-57 selectively inactivates endocannabinoid hydrolases, these experiments only evaluated enzymes from the serine hydrolase class and therefore could miss additional targets of SA-57 that belong to different protein classes. Click chemistry-ABPP (CC-ABPP)<sup>46–49</sup> can address this question by directly detecting proteins that are covalently modified by a small-molecule. CC-ABPP involves treating biological models with an alkyne analogue of the inhibitor of interest and then subjecting proteomes from these models to rhodamine-azide (Rh-N<sub>3</sub>) under copper-catalyzed azide-alkyne cycloaddition (“click chemistry”) conditions<sup>47</sup> to fluorescently label inhibitor-modified proteins. Clickable analogues of PF-7845 and SA-57 (PF-7845yne and SA-57yne, respectively) were prepared and first analyzed in mouse brain proteome to assess their target profiles by competitive-ABPP (Figure 6). The clickable probes showed similar potencies and selectivity profiles compared to their nonclickable parent inhibitors in competitive ABPP experiments (compare Figures 2 and 6). We therefore next evaluated the direct targets of PF-7845yne and SA-57yne in mice.

C57Bl/6 mice were treated with a dose range of PF-7845yne and SA-57yne (0.01–12.5 mg kg<sup>-1</sup>, i.p.) for 2 h and then sacrificed and their brain proteomes analyzed by competitive and CC-ABPP (Figure 7). The competitive ABPP profiles for each alkyne probe (Figure 7a and b) correlated well with their parent inhibitors (Figure 4), with PF-7845yne selectively inactivating FAAH at doses as low as 0.05 mg kg<sup>-1</sup> and SA-57yne showing preferential activity against FAAH at low doses (0.05–0.25 mg kg<sup>-1</sup>) and cross-reactivity with MAGL and ABHD6 at higher doses (1.25–12.5 mg kg<sup>-1</sup>). CC-ABPP confirmed that PF-7845yne displayed complete selectivity toward FAAH in mouse brain proteomes, as previously reported (Figure 7).<sup>31</sup> Consistent with our competitive ABPP analyses, the CC-ABPP profile for SA-57yne revealed direct labeling of FAAH, MAGL, and ABHD6. Interestingly, partial labeling of MAGL and ABHD6 could be detected at doses of SA-57yne as low as 0.25 mg kg<sup>-1</sup>, suggesting that this agent begins to inactivate 2-AG hydrolases at doses that are required to completely inactivate FAAH. CC-ABPP did not reveal any other major off-targets for SA-57yne with the exception of a faint 70 kDa protein in soluble mouse brain at doses of 6.25–12.5 mg kg<sup>-1</sup>. This enzyme likely represents the carboxylesterase ES-1, a common off-target of carbamates<sup>22,32,50,51</sup> that originates from contaminating blood<sup>52</sup> in the brain proteome samples. Considering that ES-1 signals were not noticeably depleted by SA-57yne in our competitive ABPP experiments (Figure 7b), we conclude that this inhibitor only partially inactivates ES-1 at high doses.

**Brain Endocannabinoid Levels in Mice Treated with SA-57 and PF-7845.** Based on our competitive and CC-ABPP data, we wondered whether SA-57, at low doses, could selectively elevate brain AEA and, at higher doses, increase

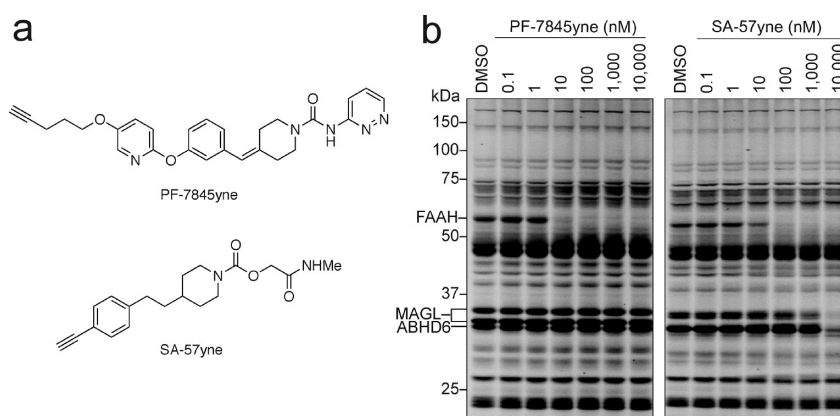


**Figure 6.** Structures (a) and in vitro competitive ABPP analysis (b) of PF-7845yne and SA-57yne in a mouse brain membrane proteome using a FP-Rh probe.

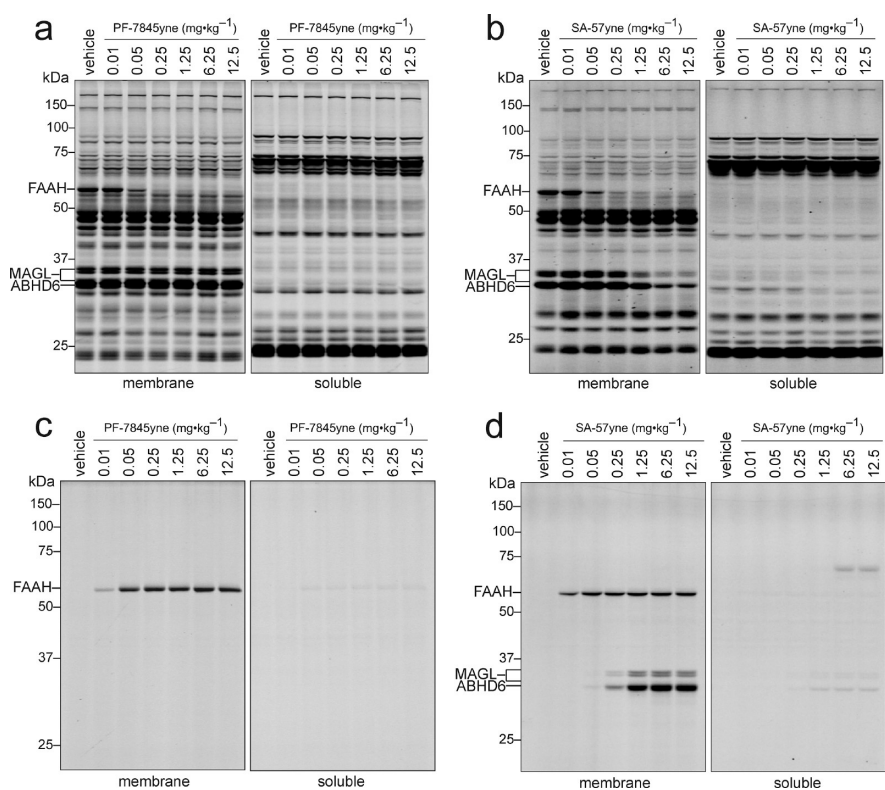


**Figure 7.** Competitive ABPP (a and b) and CC-ABPP (c and d) analysis of brain proteomes from mice treated with clickable probes PF-7845yne (a and c) and SA-57yne (b and d) at the indicated doses (0.01–12.5 mg kg<sup>-1</sup>, i.p.) for 2 h.

both AEA and 2-AG. We tested this hypothesis by measuring the levels of endocannabinoids and related lipids in brain tissue from mice treated with a dose range (0.125–12.5 mg kg<sup>-1</sup>, i.p.) of SA-57, PF-7845, or vehicle (Figure 8). Both inhibitors were found to elevate the FAAH substrates AEA, PEA, and OEA by ~10-fold across the entire tested dose-range. SA-57, but not PF-7845, also increased brain 2-AG by 3- and >10-fold at doses of 1.25 and 12.5 mg kg<sup>-1</sup>, respectively. These data are consistent with our competitive ABPP experiments, which revealed partial and near-complete inhibition of MAGL (and ABHD6) by SA-57 at doses of 1.25 and 12.5 mg kg<sup>-1</sup>, respectively. Brain arachidonic acid levels were also significantly decreased by SA-57 at 12.5 mg kg<sup>-1</sup>, as has been observed before with the selective MAGL inhibitor JZL184.<sup>21,22</sup> These data, taken together, indicate that, across a relatively narrow

(~10-fold) dose-range, SA-57 can act as either a selective FAAH inhibitor or general endocannabinoid hydrolase inhibitor in vivo.

**Conclusion.** We have found herein that the *O*-hydroxyacetamide carbamate SA-57 constitutes an unusual type of endocannabinoid hydrolase inhibitor that shows selectivity for FAAH at low concentrations and additional activity against the 2-AG hydrolases MAGL and ABHD6 at higher concentrations. Previous dual FAAH-MAGL inhibitors, like JZL195,<sup>53</sup> have tended to show similar potencies for FAAH and MAGL. We thus anticipate that SA-57 will provide a useful pharmacological probe to investigate the behavioral effects of partial MAGL inhibition on a backdrop of full FAAH blockade. We have previously reported that complete and prolonged blockade of MAGL, but not FAAH, causes behavioral tolerance associated

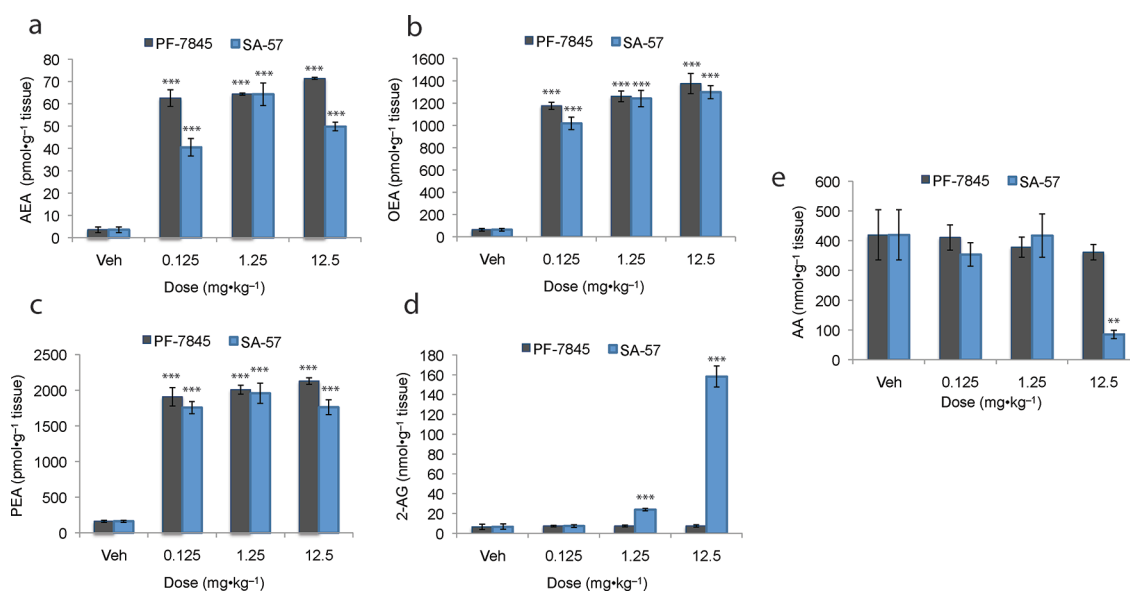


**Figure 8.** Brain lipid profile for mice treated with PF-7845, SA-57, or vehicle at indicated doses (0.125–12.5 mg kg<sup>-1</sup>, i.p.) for 2 h. \*,  $P < 0.05$ ; \*\*,  $P < 0.01$ ; \*\*\*,  $P < 0.001$  for vehicle-treated versus inhibitor-treated mice. Data are presented as means  $\pm$  SEM,  $n =$  three mice per group.

with CB1 downregulation and desensitization.<sup>24</sup> More recently, partial, chronic blockade of MAGL has been shown to produce sustained CB1-mediated behavioral effects in rodent anxiety and pain models.<sup>25,26</sup> Whether the magnitude of these effects could be further increased (and sustained) by concurrent FAAH blockade is worthy of future investigation. SA-57 offers an appropriate polypharmacologic tool to explore the neuro-behavioral effects of complete FAAH blockade in conjunction with varying degrees of MAGL and ABHD6 inhibition.

## METHODS

**Materials.** PF-7845 was prepared according to literature precedent.<sup>30,54</sup> Stock solutions of each inhibitor in dimethyl sulfoxide (DMSO) were prepared to assess in vitro potency and selectivity data. Fluorophosphonate-rhodamine (FP-Rh) was synthesized as previously described.<sup>55</sup> Silica gel chromatography was performed using the appropriate size Teledyne-Isco RediSep prepacked silica filled cartridges. High resolution mass spectrometry (HRMS) was carried out using an Agilent (6220) LC-MS TOF instrument using (3.5 pH) aqueous ammonium formate as mobile phase A1 and 50:50 methanol/acetonitrile as mobile phase B1. Low resolution mass spectral data was collected on a Micromass ADM atmospheric pressure chemical ionization instrument (LRMS APCI). NMR spectra were generated on a Varian 400 MHz or Varian 600 MHz instrument. Chemical shifts were recorded in ppm relative to tetramethylsilane (TMS) with multiplicities given as s (singlet), bs (broad singlet), d (doublet), t (triplet), dt (doublet of triplets), q (quadruplet), qd (quadruplet of doublets), m (multiplet). All target compounds were analyzed using ultrahigh performance liquid chromatography/UV/evaporative light scattering detection coupled to time-of-flight mass spectrometry (UHPLC/UV/ELSD/TOFMS) and were found to be >95% pure. The UHPLC was performed on a Waters ACQUITY UHPLC system (Waters, Milford, MA), which was equipped with a binary solvent delivery manager, column manager, and sample manager coupled to ELSD and UV detectors (Waters, Milford, MA). Detection was performed on a Waters LCT premier XE mass spectrometer (Waters, Milford, MA). The instrument was fitted with an Acquity BEH (bridged ethane hybrid) C18 column (30 mm  $\times$  2.1 mm, 1.7  $\mu$ m particle size, Waters, Milford, MA) operated at 60  $^{\circ}$ C.

**Synthesis of SA-57 and SA-57yne.** 2-Methoxy-2-oxoethyl 4-(4-chlorophenethyl)piperidine-1-carboxylate (**3**). Methyl 2-((phenoxy-carbonyl)oxy)acetate (1.01 g, 4.80 mmol, 1.25 equiv), 4-(4-chlorophenethyl)piperidine (1.00 g, 3.84 mmol,

1.0 equiv), and diisopropylethylamine (0.84 mL, 4.80 mmol, 1.25 equiv) were combined in DMSO (5 mL) and heated to 80  $^{\circ}$ C for 24 h. The reaction was cooled to room temperature and partitioned between EtOAc and water. The organic layer was dried over MgSO<sub>4</sub>, filtered, and concentrated to a thick oil which was purified by silica gel chromatography (5% EtOAc in heptane to 100% EtOAc) to provide carbamate **3** as a thick brown oil (1.22 g, 93%). <sup>1</sup>H NMR (400 MHz, CDCl<sub>3</sub>)  $\delta$  1.14–1.27 (m, 2H), 1.39–1.53 (m, 1 H), 1.53–1.61 (m, 2H), 1.74 (d,  $J = 12.1$  Hz, 2H), 2.57–2.66 (m, 2H), 2.68–2.93 (m, 2H), 3.77 (s, 3 H), 4.17 (d,  $J = 12.1$  Hz, 2H), 4.62 (s, 2H), 7.07–7.13 (m, 2H), 7.23–7.27 (m, 2H); MS (APCI)  $M^+ = 339.9$ .

2-(Methylamino)-2-oxoethyl 4-(4-chlorophenethyl)piperidine-1-carboxylate (SA-57). To a solution of carbamate **3** (1.2 g, 3.5 mmol) in DMSO (15 mL) was added methylamine (17.7 mL of a 2 M tetrahydrofuran (THF) solution, 35 mmol, 10 equiv). The reaction vessel was sealed, and the solution was stirred at room temperature for 5 days. The reaction was partitioned between MTBE and water, and the organic layer was dried over MgSO<sub>4</sub>, filtered, and concentrated. The resulting residue was purified by silica gel chromatography (EtOAc) to provide SA-57 as a white solid (0.989 g, 83%). <sup>1</sup>H NMR (400 MHz, CDCl<sub>3</sub>)  $\delta$  1.19 (qd,  $J = 12.3, 4.5$  Hz, 2 H), 1.41–1.53 (m, 1 H), 1.54–1.62 (m, 2 H), 1.77 (d,  $J = 12.5$  Hz, 2 H), 2.57–2.67 (m, 2 H), 2.70–2.86 (m, 2 H), 2.88 (d,  $J = 4.9$  Hz, 3 H), 4.04–4.27 (m, 2 H), 4.52–4.69 (m, 2 H), 6.06 (bs, 1 H), 7.07–7.14 (m, 2 H), 7.23–7.27 (m, 2 H); <sup>13</sup>C NMR (100 MHz, CDCl<sub>3</sub>)  $\delta$  25.9, 31.7, 32.1, 32.2, 35.2, 38.0, 44.4, 64.2, 128.5, 129.6, 131.5, 140.6, 154.0, 168.7; MS (APCI)  $M^+ = 338.9$ .

2-(Methylamino)-2-oxoethyl 4-(4-((triethylsilyl)ethynyl)phenethyl)piperidine-1-carboxylate. SA-57 (590 mg, 1.74 mmol, 1 equiv), bis(acetonitrile)palladium(II) chloride (23 mg, 0.087 mmol, 0.05 equiv), X-Phos (85 mg, 0.174 mmol, 0.1 equiv), and Cs<sub>2</sub>CO<sub>3</sub> (851 mg, 2.61 mmol, 1.5 equiv) were placed in a 50 mL round-bottom flask. The vessel was evacuated and backfilled with N<sub>2</sub> (3 $\times$ ). Acetonitrile (10 mL) was added and the mixture stirred for 25 min at room temperature. Triethylsilylacetylene (0.468 mL, 2.61 mmol, 1.5 equiv) was added to the mixture, and the reaction was heated to 85  $^{\circ}$ C for 4 h and then stirred at room temperature overnight. The mixture was partitioned between water and EtOAc. The organic layer was dried over MgSO<sub>4</sub>, filtered, and concentrated. The resulting residue was purified by silica gel chromatography (50% EtOAc in heptane to 100% EtOAc) to provide the title compound as a tan solid (690 mg, 89%). <sup>1</sup>H NMR (400 MHz, CDCl<sub>3</sub>)  $\delta$  0.68 (q, 6 H), 1.05 (t,  $J = 7.9$  Hz, 9 H), 1.19 (qd,  $J = 12.3, 4.5$  Hz, 2 H), 1.41–1.53 (m, 1 H), 1.54–1.62



(m, 2 H), 1.77 (d,  $J = 12.5$  Hz, 2 H), 2.57–2.67 (m, 2 H), 2.70–2.86 (m, 2 H), 2.88 (d,  $J = 4.9$  Hz, 3 H), 4.04–4.27 (m, 2 H), 4.52–4.69 (m, 2 H), 6.06 (bs, 1 H), 7.07–7.14 (m, 2 H), 7.38–7.42 (m, 2 H); MS (APCI)  $M^+ = 443.2$ .

**2-(Methylamino)-2-oxoethyl 4-(4-ethynylphenethyl)piperidine-1-carboxylate (SA-57yne).** 2-(Methylamino)-2-oxoethyl 4-(4-((triethylsilyl)ethynyl)phenethyl)piperidine-1-carboxylate (690 mg, 1.56 mmol, 1.0 equiv) was dissolved in THF (10 mL) and cooled in an ice bath. TBAF (1.72 mL of 1.0 M solution in THF, 1.72 mmol, 1.1 equiv) was added, and the reaction was stirred at 0 °C for 1 h. The mixture was partitioned between water and EtOAc. The organic layer was dried over  $MgSO_4$ , filtered, and concentrated. The resulting residue was purified by silica gel chromatography (20% acetone in heptane to 50% acetone in heptane) to provide SA-57yne as a white solid (194 mg, 38%).  $^1H$  NMR (400 MHz,  $CDCl_3$ )  $\delta$  1.12–1.26 (m, 1 H), 1.39–1.53 (m, 1 H), 1.55–1.64 (m, 1 H), 1.77 (d,  $J = 11.5$  Hz, 1 H), 2.61–2.71 (m, 1 H), 2.72–2.86 (m, 1 H), 2.88 (d,  $J = 5.1$  Hz, 1 H), 3.05 (s, 1 H), 4.03–4.26 (m, 2 H), 4.49–4.67 (m, 2 H), 6.06 (bs, 1 H), 7.13 (d,  $J = 8.2$  Hz, 1 H), 7.42 (d,  $J = 7.8$  Hz, 1 H);  $^{13}C$  NMR (150 MHz,  $CDCl_3$ )  $\delta$  25.9, 31.6, 32.1, 32.8, 35.2, 37.8, 44.4, 64.2, 76.7, 83.6, 119.5, 128.3, 132.2, 143.2, 154.0, 168.7; MS (APCI)  $M^+ = 328.8$ .

**Synthesis of PF-7845yne.** *tert*-Butyl 4-(3-((5-((5-trimethylsilyl)pent-4-yn-1-yloxy)pyridin-2-yl)oxy)benzylidene)piperidine-1-carboxylate. To a solution of *tert*-butyl 4-(3-((5-hydroxypyridin-2-yl)oxy)benzylidene)piperidine-1-carboxylate (0.8 g, 2.09 mmol; see Example 47 in WO 2008/047229)<sup>54</sup> in DMF (5 mL) was added 5-trimethylsilyl-4-pentyn-1-iodide (0.696 g, 2.6 mmol),  $K_2CO_3$  (0.57 g, 4.18 mmol), and 18-crown-6 ether (0.87 g, 4.18 mmol) at room temperature. The reaction mixture was stirred at room temperature overnight. The mixture was diluted with water (10 mL), and the mixture was extracted with ethyl acetate. The organic layer was washed with water and brine, dried over  $Na_2SO_4$ , and concentrated under reduced pressure. Purification by silica gel column chromatography (1:4 acetone/hexanes) afforded the pure title compound (0.7 g, 64%).  $^1H$  NMR (500 MHz,  $CDCl_3$ )  $\delta$  7.88 (d,  $J = 2.5$  Hz, 1 H), 7.29 (d,  $J = 8.1$  Hz, 2 H), 6.97 (d,  $J = 7.8$  Hz, 1 H), 6.91 (d,  $J = 9.6$  Hz, 2 H), 6.85 (d,  $J = 8.8$  Hz, 1 H), 6.32 (s, 1 H), 4.06 (t,  $J = 6$  Hz, 2 H), 3.49 (s, 2 H), 3.39 (s, 2 H), 2.43 (t,  $J = 6.9$  Hz, 4 H), 2.31 (s, 2 H), 1.97 (t,  $J = 6.4$  Hz, 2 H), 1.47 (s, 9 H), 0.14 (s, 9 H).

*tert*-Butyl 4-(3-((5-(*pent*-4-yn-1-yloxy)pyridin-2-yl)oxy)benzylidene)piperidine-1-carboxylate. To a solution of *tert*-butyl 4-(3-((5-((5-trimethylsilyl)pent-4-yn-1-yloxy)pyridin-2-yl)oxy)benzylidene)piperidine-1-carboxylate (0.7 g, 1.34 mmol) in dry THF (4 mL) cooled to 0 °C was added TBAF (3.8 mL, 13.4 mmol) dropwise. The mixture was stirred for 30 min. The reaction was concentrated, and the residue was partitioned between saturated  $NaHCO_3$  solution and  $CH_2Cl_2$ . The organic layer was dried over  $Na_2SO_4$  and concentrated to give the title compound (0.6 g, 98% yield).

**5-(*Pent*-4-yn-1-yloxy)-2-(3-(piperidin-4-ylidenemethyl)phenoxy)pyridine.** To a solution of *tert*-butyl 4-(3-((5-(*pent*-4-yn-1-yloxy)pyridin-2-yl)oxy)benzylidene)piperidine-1-carboxylate (0.68 g, 1.33 mmol) dry  $CH_2Cl_2$  (3 mL) cooled to 0 °C was added TFA (1 mL, 13.3 mmol) dropwise. The mixture was stirred for 30 min. The reaction was concentrated, and the residue was partitioned between saturated  $NaHCO_3$  solution and  $CH_2Cl_2$ . The organic layer was dried over  $Na_2SO_4$  and concentrated to give the title compound (0.53 g, 99% yield). MS (APCI)  $M^+ = 421.2$ .

**4-(3-((5-(*Pent*-4-yn-1-yloxy)pyridin-2-yl)oxy)benzylidene)-*N*-(pyridazin-3-yl)piperidine-1-carboxamide (PF-7845yne).** To a solution of 5-(*pent*-4-yn-1-yloxy)-2-(3-(piperidin-4-ylidenemethyl)phenoxy)pyridine (0.26 g, 0.746 mmol) and phenyl pyridazinyl carbamate (0.16 g, 0.746 mmol) in DMSO (3 mL) was added triethylamine (0.3 mL), and the reaction mixture was stirred for 12 h at room temperature. The reaction mixture was diluted with water and extracted with ethyl acetate. The organic layer was washed with water, dried over  $Na_2SO_4$ , and concentrated. Purification by silica gel column chromatography (2:5 acetone/hexanes) afforded the pure title compound (0.225 g,

64%).  $^1H$  NMR (500 MHz,  $CDCl_3$ )  $\delta$  8.77 (s, 1 H), 8.40 (s, 1 H), 7.89 (s, 1 H), 7.46 (t,  $J = 4.5$  Hz, 1 H), 7.29 (m, 2 H), 6.98 (d,  $J = 7.5$  Hz, 1 H), 6.92 (m, 2 H), 6.87 (d,  $J = 8.75$  Hz, 1 H), 6.40 (s, 1 H), 4.08 (t,  $J = 5.75$  Hz, 2 H), 3.70 (m, 2 H), 3.59 (m, 2 H), 2.60 (d,  $J = 5.2$  Hz, 2 H), 2.47 (m, 2 H), 2.40 (t,  $J = 6.6$  Hz, 2 H), 1.99 (m, 3 H);  $^{13}C$  NMR (125 MHz,  $CDCl_3$ )  $\delta$  157.5, 156.6, 155.2, 151.8, 138.7, 137.5, 133.7, 129.4, 128.2, 126.8, 125.0, 124.6, 120.6, 118.4, 112.52, 83.1, 69.1, 67.3, 45.7, 44.6, 35.8, 29.1, 28.1, 15.1; MS (APCI)  $M^+ = 470.2$ .

**Preparation of Mouse Brain Proteomes from Inhibitor-Treated Mice.** Inhibitors were intraperitoneally administered to C57Bl/6J mice in a vehicle of ethanol/emulphor/saline (1:1:18), and, after the indicated times, the animals were anesthetized using isoflurane and sacrificed by decapitation and tissues were immediately dissected. Mouse brains were harvested, hemisected, and frozen in liquid  $N_2$ . Each half brain was washed with cold phosphate-buffered saline at 0 °C ( $2 \times 1$  mL) to remove excess blood and immediately dounce homogenized in PBS (1 mL). Dounced tissue was sonicated and centrifuged (1000g, 10 min, 4 °C) to remove cellular debris. The supernatant was centrifuged at high speed (100 000g, 45 min, 4 °C) to separate membrane and soluble cell components. The supernatant was saved as the soluble fraction. The remaining pellet was gently washed with cold PBS ( $2 \times$ , 500  $\mu$ L) and sonicated in PBS (300  $\mu$ L) to resuspend. Total protein concentrations of the soluble and membrane fractions were determined using the Bio-Rad DC Protein Assay kit. Proteomic mixtures were either diluted to 1.0 mg/mL total protein concentration with PBS for immediate use or aliquoted and stored at -80 °C. The studies were performed with the approval of the Institutional Animal Care and Use Committee at The Scripps Research Institute in accordance with the Guide for the Care and Use of Laboratory Animals.

**Recombinant Expression of Human and Mouse FAAH, MAGL, and ABHD6 in HEK293 Cells.** All forms of serine hydrolases (mFAAH, hFAAH, mMAGL, hMAGL, and mABHD6) were expressed according to previously reported methods.<sup>43</sup> Full-length cDNAs encoding mouse and human FAAH, MAGL, and ABHD6 were subcloned into pcDNA3 (Invitrogen). HEK293 cells were grown to approximately 70% confluence in 100 mm dishes using complete medium (DMEM with L-glutamine, nonessential amino acids, sodium pyruvate, and FCS) at 37 °C and 5%  $CO_2$ . To each dish containing HEK293 cells was added 4  $\mu$ g of appropriate cDNA or empty vector control ("mock") and 12  $\mu$ L FuGene 6 solution (Roche Applied Science). Cells were harvested 48 h later by aspirating off media, washing twice with PBS, and scraping. Cells were spun (1400 rpm, 3 min), supernatant removed, and cells reconstituted in 500  $\mu$ L PBS. Cell lysates were diluted to 0.1 mg/mL protein concentration for use in competitive ABPP experiments.

**In Vitro Competitive ABPP with FAAH Inhibitors.** Membrane or soluble proteomes (50  $\mu$ L, 1.0 mg/mL total protein concentration) were preincubated with varying concentrations of inhibitors at 37 °C. After 30 min, FP-Rh (1.0  $\mu$ L, 50  $\mu$ M in DMSO) was added, and the mixture was incubated for another 30 min at 37 °C. Reactions were quenched with SDS loading buffer (50  $\mu$ L, 4 $\times$ ) and run on SDS-PAGE.

**In Vitro CC ABPP with FAAH Inhibitors.** Click chemistry labeling of PF-7845yne and SA-57yne-labeled targets with Rh- $N_3$  was performed according to previously reported methods.<sup>32</sup> Briefly,  $CuSO_4$  (1.0  $\mu$ L/reaction, 50 mM in  $H_2O$ ), TBTA (3.0  $\mu$ L/reaction, 1.7 mM in DMSO/*t*-BuOH [1:4]), TCEP (1.0  $\mu$ L/reaction, 50 mM in  $H_2O$  [freshly prepared]) and Rh- $N_3$  (1.0  $\mu$ L/reaction, 1.25 mM in DMSO) were premixed. This click reagent cocktail (6.0  $\mu$ L) was immediately added to brain proteomes (50  $\mu$ L, 1.0 mg/mL protein concentration) from inhibitor or vehicle treated mice, and the reaction stirred by briefly vortexing. After 1 h at room temperature, reactions were diluted with SDS loading buffer (50  $\mu$ L, 4 $\times$ ) and immediately run on SDS-PAGE.

**Measurement of Brain Lipids.** Brain lipid levels were determined according to previously reported methods.<sup>22</sup>

## ■ AUTHOR INFORMATION

## Corresponding Author

\*E-mail: cravatt@scripps.edu.

## Funding

This work was supported by the NIH (DA017259 (BFC), DA009789 (BFC), DA032541-01 (MJN)) and the Skaggs Institute for Chemical Biology.

## ■ REFERENCES

- (1) Ligresti, A., Petrosino, S., and Di Marzo, V. (2009) From endocannabinoid profiling to 'endocannabinoid therapeutics'. *Curr. Opin. Chem. Biol.* 13, 321–331.
- (2) Di Marzo, V. (2008) Targeting the endocannabinoid system: to enhance or reduce? *Nat. Rev. Drug Discovery* 7, 438–455.
- (3) Fowler, C. J. (2008) "The tools of the trade"—an overview of the pharmacology of the endocannabinoid system. *Curr. Pharm. Des.* 14, 2254–2265.
- (4) Graham, E. S., Ashton, J. C., and Glass, M. (2009) Cannabinoid receptors: A brief history and "what's hot". *Front. Biosci.* 14, 944–957.
- (5) Ahn, K., McKinney, M. K., and Cravatt, B. F. (2008) Enzymatic pathways that regulate endocannabinoid signaling in the nervous system. *Chem. Rev.* 108, 1687–1707.
- (6) Cravatt, B. F., and Lichtman, A. H. (2003) Fatty acid amide hydrolase: an emerging therapeutic target in the endocannabinoid system. *Curr. Opin. Chem. Biol.* 7, 469–475.
- (7) Gaetani, S., Cuomo, V., and Piomelli, D. (2003) Anandamide hydrolysis: a new target for anti-anxiety drugs? *Trends Mol. Med.* 9, 474–478.
- (8) Cravatt, B. F., Demarest, K., Patricelli, M. P., Bracey, M. H., Giang, D. K., Martin, B. R., and Lichtman, A. H. (2001) Supersensitivity to anandamide and enhanced endogenous cannabinoid signaling in mice lacking fatty acid amide hydrolase. *Proc. Natl. Acad. Sci. U.S.A.* 98, 9371–9376.
- (9) Lichtman, A. H., Leung, D., Shelton, C. C., Saghatelian, A., Hardouin, C., Boger, D. L., and Cravatt, B. F. (2004) Reversible inhibitors of fatty acid amide hydrolase that promote analgesia: Evidence for an unprecedented combination of potency and selectivity. *J. Pharmacol. Exp. Ther.* 311, 441–448.
- (10) Booker, L., Kinsey, S. G., Abdullah, R. A., Blankman, J. L., Long, J. Z., Ezzili, C., Boger, D. L., Cravatt, B. F., and Lichtman, A. H. (2011) The FAAH inhibitor PF-3845 acts in the nervous system to reverse lipopolysaccharide-induced tactile allodynia in mice. *Br. J. Pharmacol.* DOI: 10.1111/j.1476-5381.2011.001445.x.
- (11) Lichtman, A. H., Shelton, C. C., Advani, T., and Cravatt, B. F. (2004) Mice lacking fatty acid amide hydrolase exhibit a cannabinoid receptor-mediated phenotypic hypoalgesia. *Pain* 109, 319–327.
- (12) Kathuria, S., Gaetani, S., Fegley, D., Valino, F., Duranti, A., Tontini, A., Mor, M., Tarzia, G., La Rana, G., Calignano, A., Giustino, A., Tattoli, M., Palmery, M., Cuomo, V., and Piomelli, D. (2003) Modulation of anxiety through blockade of anandamide hydrolysis. *Nat. Med.* 9, 76–81.
- (13) Chang, L., Luo, L., Palmer, J. A., Sutton, S., Wilson, S. J., Barbier, A. J., Breitenbucher, J. G., Chaplan, S. R., and Webb, M. (2006) Inhibition of fatty acid amide hydrolase produces analgesia by multiple mechanisms. *Br. J. Pharmacol.* 148, 102–113.
- (14) Russo, R., LoVerme, J., La Rana, G., Compton, T. R., Parrott, J., Duranti, A., Tontini, A., Mor, M., Tarzia, G., Calignano, A., and Piomelli, D. (2007) The fatty acid amide hydrolase inhibitor URBS97 (cyclohexylcarbamic acid 3'-carbamoylebiphenyl-3-yl ester) reduces neuropathic pain after oral administration in mice. *J. Pharmacol. Exp. Ther.* 322, 236–242.
- (15) Cravatt, B. F., Saghatelian, A., Hawkins, E. G., Clement, A. B., Bracey, M. H., and Lichtman, A. H. (2004) Functional disassociation of the central and peripheral fatty acid amide signaling systems. *Proc. Natl. Acad. Sci. U.S.A.* 101, 10821–10826.
- (16) Massa, F., Marsicano, G., Hermann, H., Cannich, A., Monory, K., Cravatt, B. F., Ferri, G.-L., Sibaev, A., Storr, M., and Lutz, B. (2004) The endogenous cannabinoid system protects against colonic inflammation. *J. Clin. Invest.* 113, 1202–1209.
- (17) Holt, S., Comelli, F., Costa, B., and Fowler, C. J. (2005) Inhibitors of fatty acid amide hydrolase reduce carrageenan-induced hind paw inflammation in pentobarbital-treated mice: comparison with indomethacin and possible involvement of cannabinoid receptors. *Br. J. Pharmacol.* 146, 467–476.
- (18) Naidu, P., Varvel, S., Ahn, K., Cravatt, B., Martin, B., and Lichtman, A. (2007) Evaluation of fatty acid amide hydrolase inhibition in murine models of emotionality. *Psychopharmacology* 192, 61–70.
- (19) Moreira, F. A., Kaiser, N., Monory, K., and Lutz, B. (2008) Reduced anxiety-like behaviour induced by genetic and pharmacological inhibition of the endocannabinoid-degrading enzyme fatty acid amide hydrolase (FAAH) is mediated by CB1 receptors. *Neuropharmacology* 54, 141–150.
- (20) Gobbi, G., Bambico, F. R., Mangieri, R., Bortolato, M., Campolongo, P., Solinas, M., Cassano, T., Morgese, M. G., Debonnel, G., Duranti, A., Tontini, A., Tarzia, G., Mor, M., Trezza, V., Goldberg, S. R., Cuomo, V., and Piomelli, D. (2005) Antidepressant-like activity and modulation of brain monoaminergic transmission by blockade of anandamide hydrolysis. *Proc. Natl. Acad. Sci. U.S.A.* 102, 18620–18625.
- (21) Long, J. Z., Li, W., Booker, L., Burston, J. J., Kinsey, S. G., Schlosburg, J. E., Pavon, F. J., Serrano, A. M., Selley, D. E., Parsons, L. H., Lichtman, A. H., and Cravatt, B. F. (2009) Selective blockade of 2-arachidonoylglycerol hydrolysis produces cannabinoid behavioral effects. *Nat. Chem. Biol.* 5, 37–44.
- (22) Long, J. Z., Nomura, D. K., and Cravatt, B. F. (2009) Characterization of monoacylglycerol lipase inhibition reveals differences in central and peripheral endocannabinoid metabolism. *Chem. Biol.* 16, 744–753.
- (23) Long, J. Z., Nomura, D. K., Vann, R. E., Walentiny, D. M., Booker, L., Jin, X., Burston, J. J., Sim-Selley, L. J., Lichtman, A. H., Wiley, J. L., and Cravatt, B. F. (2009) Dual blockade of FAAH and MAGL identifies behavioral processes regulated by endocannabinoid crosstalk in vivo. *Proc. Natl. Acad. Sci. U.S.A.* 106, 20270–20275.
- (24) Schlosburg, J. E., Blankman, J. L., Long, J. Z., Nomura, D. K., Pan, B., Kinsey, S. G., Nguyen, P. T., Ramesh, D., Booker, L., Burston, J. J., Thomas, E. A., Selley, D. E., Sim-Selley, L. J., Liu, Q. S., Lichtman, A. H., and Cravatt, B. F. (2010) Chronic monoacylglycerol lipase blockade causes functional antagonism of the endocannabinoid system. *Nat. Neurosci.* 13, 1113–1119.
- (25) Sciolino, N. R., Zhou, W., and Hohmann, A. G. (2011) Enhancement of endocannabinoid signaling with JZL184, an inhibitor of the 2-arachidonoylglycerol hydrolyzing enzyme monoacylglycerol lipase, produces anxiolytic effects under conditions of high environmental aversiveness in rats. *Pharmacol. Res.* 64, 226–234.
- (26) Busquets-Garcia, A., Puighermanal, E., Pastor, A., de la Torre, R., Maldonado, R., and Ozaita, A. S. (2011) Differential role of anandamide and 2-arachidonoylglycerol in memory and anxiety-like responses. *Biol. Psychiatry* 70, 479–486.
- (27) Otrubova, K., Ezzili, C., and Boger, D. L. (2011) The discovery and development of inhibitors of fatty acid amide hydrolase (FAAH). *Bioorg. Med. Chem. Lett.* 21, 4674–4685.
- (28) Ahn, K., Johnson, D. S., and Cravatt, B. F. (2009) Fatty acid amide hydrolase as a potential therapeutic target for the treatment of pain and CNS disorders. *Expert Opin. Drug Discovery* 4, 763–784.
- (29) Koutek, B., Prestwich, G. D., Howlett, A. C., Chin, S. A., Salehani, D., Akhavan, N., and Deutsch, D. G. (1994) Inhibitors of arachidonoyl ethanolamide hydrolysis. *J. Biol. Chem.* 269, 22937–22940.
- (30) Johnson, D. S., Stiff, C., Lazerwith, S. E., Kesten, S. R., Fay, L. K., Morris, M., Beidler, D., Liimatta, M. B., Smith, S. E., Dudley, D. T., Sadagopan, N., Bhattachar, S. N., Kesten, S. J., Nomanbhoy, T. K., Cravatt, B. F., and Ahn, K. (2010) Discovery of PF-04457845: A highly potent, orally bioavailable, and selective urea FAAH inhibitor. *ACS Med. Chem. Lett.* 2, 91–96.



- (31) Ahn, K., Smith, S. E., Liimatta, M. B., Beidler, D., Sadagopan, N., Dudley, D. T., Young, T., Wren, P., Zhang, Y., Swaney, S., Van Becelaere, K., Blankman, J. L., Nomura, D. K. K., Bhattachar, S. N., Stiff, C., Nomanbhoy, T. K., Weerapana, E., Johnson, D. S., and Cravatt, B. F. (2011) Mechanistic and pharmacological characterization of PF-04457845: a highly potent and selective FAAH inhibitor that reduces inflammatory and noninflammatory pain. *J. Pharmacol. Exp. Ther.* 338, 114–124.
- (32) Alexander, J. P., and Cravatt, B. F. (2005) Mechanism of carbamate inactivation of FAAH: Implications for the design of covalent inhibitors and in vivo functional probes for enzymes. *Chem. Biol.* 12, 1179–1187.
- (33) Alexander, J. P., and Cravatt, B. F. (2006) The putative endocannabinoid transport blocker LY2183240 is a potent inhibitor of FAAH and several other brain serine hydrolases. *J. Am. Chem. Soc.* 128, 9699–9704.
- (34) Ahn, K., Johnson, D. S., Mileni, M., Beidler, D., Long, J. Z., McKinney, M. K., Weerapana, E., Sadagopan, N., Liimatta, M., Smith, S. E., Lazerwith, S., Stiff, C., Kamtekar, S., Bhattacharya, K., Zhang, Y., Swaney, S., Van Becelaere, K., Stevens, R. C., and Cravatt, B. F. (2009) Discovery and characterization of a highly selective FAAH inhibitor that reduces inflammatory pain. *Chem. Biol.* 16, 411–420.
- (35) Mileni, M., Kamtekar, S., Wood, D. C., Benson, T. E., Cravatt, B. F., and Stevens, R. C. (2010) Crystal Structure of Fatty Acid Amide Hydrolase Bound to the Carbamate Inhibitor URB597: Discovery of a Deacylating Water Molecule and Insight into Enzyme Inactivation. *J. Mol. Biol.* 400, 743–754.
- (36) Mileni, M., Johnson, D. S., Wang, Z., Everdeen, D. S., Liimatta, M., Pabst, B., Bhattacharya, K., Nugent, R. A., Kamtekar, S., Cravatt, B. F., Ahn, K., and Stevens, R. C. (2008) Structure-guided inhibitor design for human FAAH by interspecies active site conversion. *Proc. Natl. Acad. Sci. U.S.A.* 105, 12820–12824.
- (37) Tarzia, G., Duranti, A., Gatti, G., Piersanti, G., Tontini, A., Rivara, S., Lodola, A., Plazzi, P. V., Mor, M., Kathuria, S., and Piomelli, D. (2006) Synthesis and structure–activity relationships of FAAH inhibitors: Cyclohexylcarbamic acid biphenyl esters with chemical modulation at the proximal phenyl ring. *ChemMedChem* 1, 130–139.
- (38) Abouabdellah, A., Almario, G. A., Hoornaert, C., Lardenois, P., and Marguet, F. (2005) Aryl- and heteroaryl-piperidinecarboxylate derivatives, their preparation and use as fatty acid amide hydrolase (FAAH) inhibitors for treating FAAH-related pathologies, US 2007/0021405, 31 pp, Sanofi-Synthelabo, France.
- (39) Leung, D., Hardouin, C., Boger, D. L., and Cravatt, B. F. (2003) Discovering potent and selective reversible inhibitors of enzymes in complex proteomes. *Nat. Biotechnol.* 21, 687–691.
- (40) Gelman, D., and Buchwald, S. L. (2003) Efficient palladium-catalyzed coupling of aryl chlorides and tosylates with terminal alkynes: use of a copper cocatalyst inhibits the reaction. *Angew. Chem., Int. Ed.* 42, 5993–5996.
- (41) Jessani, N., Liu, Y., Humphrey, M., and Cravatt, B. F. (2002) Enzyme activity profiles of the secreted and membrane proteome that depict cancer cell invasiveness. *Proc. Natl. Acad. Sci. U.S.A.* 99, 10335–10340.
- (42) Patricelli, M. P., Giang, D. K., Stamp, L. M., and Burbaum, J. J. (2001) Direct visualization of serine hydrolase activities in complex proteome using fluorescent active site-directed probes. *Proteomics* 1, 1067–1071.
- (43) Blankman, J. L., Simon, G. M., and Cravatt, B. F. (2007) A comprehensive profile of brain enzymes that hydrolyze the endocannabinoid 2-arachidonoylglycerol. *Chem. Biol.* 14, 1347–1356.
- (44) Marrs, W. R., Blankman, J. L., Horne, E. A., Thomazeau, A., Lin, Y. H., Coy, J., Bodor, A. L., Muccioli, G. G., Hu, S. S., Woodruff, G., Fung, S., Lafourcade, M., Alexander, J. P., Long, J. Z., Li, W., Xu, C., Moller, T., Mackie, K., Manzoni, O. J., Cravatt, B. F., and Stella, N. (2010) The serine hydrolase ABHD6 controls the accumulation and efficacy of 2-AG at cannabinoid receptors. *Nat. Neurosci.* 13, 951–957.
- (45) Ahn, K., Johnson, D. S., Fitzgerald, L. R., Liimatta, M., Arendse, A., Stevenson, T., Lund, E. T., Nugent, R. A., Nomanbhoy, T. K., Alexander, J. P., and Cravatt, B. F. (2007) Novel mechanistic class of fatty acid amide hydrolase inhibitors with remarkable selectivity. *Biochemistry* 46, 13019–13030.
- (46) Speers, A. E., Adam, G. C., and Cravatt, B. F. (2003) Activity-based protein profiling in vivo using a copper(I)-catalyzed azide-alkyne [3 + 2] cycloaddition. *J. Am. Chem. Soc.* 125, 4686–4687.
- (47) Speers, A. E., and Cravatt, B. F. (2004) Profiling enzyme activities in vivo using click chemistry methods. *Chem. Biol.* 11, 535–546.
- (48) Adibekian, A., Martin, B. R., Wang, C., Hsu, K.-L., Bachovchin, D. A., Niessen, S., Hoover, H., and Cravatt, B. F. (2011) Click-generated triazole ureas as ultrapotent in vivo-active serine hydrolase inhibitors. *Nat. Chem. Biol.* 7, 469–478.
- (49) Johnson, D. S., Weerapana, E., and Cravatt, B. F. (2010) Strategies for discovering and derisking covalent, irreversible enzyme inhibitors. *Future Med. Chem.* 2, 949–964.
- (50) Chang, J. W., Nomura, D. K., and Cravatt, B. F. (2011) A potent and selective inhibitor of KIAA1363/AADACL1 that impairs prostate cancer pathogenesis. *Chem. Biol.* 18, 476–484.
- (51) Bachovchin, D. A., Ji, T., Li, W., Simon, G. M., Blankman, J. L., Adibekian, A., Hoover, H., Niessen, S., and Cravatt, B. F. (2010) Superfamily-wide portrait of serine hydrolase inhibition achieved by library-versus-library screening. *Proc. Natl. Acad. Sci. U.S.A.* 107, 20941–20946.
- (52) Krishnasamy, S., Teng, A. L., Dhand, R., Schultz, R. M., and Gross, N. J. (1998) Molecular cloning, characterization, and differential expression pattern of mouse lung surfactant convertase. *Am. J. Physiol.* 275, L969–975.
- (53) Long, J. Z., Jin, X., Adibekian, A., Li, W., and Cravatt, B. F. (2010) Characterization of tunable piperidine and piperazine carbamates as inhibitors of endocannabinoid hydrolases. *J. Med. Chem.* 53, 1830–1842.
- (54) Fay, L. K., Johnson, D. S., Lazerwith, S. E., Morris, M. A., Wang, L. J., Meyers, M. J., Kesten, S. R., and Stiff, C. M. (2008) Preparation of (hetero)biaryl ether methylenepiperidinyl ureas as fatty acid amide hydrolase (FAAH) inhibitors, WO 2008/047229, 126 pp, Pfizer Products Inc., USA.
- (55) Liu, Y., Patricelli, M. P., and Cravatt, B. F. (1999) Activity-based protein profiling: The serine hydrolases. *Proc. Natl. Acad. Sci. U.S.A.* 96, 14694–14699.